InAs quantum dots grown on the GaAs(113)*A* and GaAs($\overline{113}$)*B* surfaces: A comparative STM study

Y. Temko, T. Suzuki, P. Kratzer, and K. Jacobi*
Fritz-Haber-Institut der Max-Planck-Gesellschaft, Faradayweg 4–6, D-14195 Berlin, Germany
(Received 7 May 2003; published 14 October 2003)

InAs quantum dots (QD's) were grown on GaAs(113)*A* and GaAs($\overline{113}$)*B* substrates by molecular-beam epitaxy. Atomically resolved scanning tunneling microscopy images acquired *in situ* from uncapped samples reveal the shape of the QD's including the atomic structure of their main bounding facets. On the (113)*A* substrate the QD's are elongated along $[33\overline{2}]$ with a wide size distribution, whereas on ($\overline{113}$)*B* they are rather round and exhibit a more uniform size distribution. These observations are related to the different morphology of the substrates before QD formation. The differences in shape, size, and size distribution are discussed in terms of facet growth kinetics.

DOI: 10.1103/PhysRevB.68.165310 PACS number(s): 68.65.Hb, 68.37.Ef, 81.05.Ea, 68.35.Bs

I. INTRODUCTION

Dislocation-free three-dimensional (3D) islands, called quantum dots (QD's), have attracted considerable interest recently because they behave like artificial atoms with unique optoelectronic properties.[1,2] The QD's grow in the Stranski-Krastanow (SK) growth mode,[3] which often occurs in heteroepitaxy for systems with significant lattice mismatch such as InAs/GaAs (7.2%). The SK growth mode leads to an instantaneous self-organization of the QD's on top of a wetting layer, when the amount of deposited material exceeds a critical thickness which is about 1.6 monolayer (ML) for InAs/GaAs(001). The QD's, composed of a low-band-gap semiconductor (e.g., InAs or $In_xGa_{1-x}As$) and embedded in a wide-band-gap substrate (e.g., GaAs), create a confinement potential for electrons and holes. Thereby, the electronic structure of the QD's and the efficiency of the devices based on them are determined by their shape, size, and size distribution which presumably are largely fixed during the SK growth mode.

It has been known for some time that the reconstruction and orientation of the substrate play a key role in InAs/GaAs heteroepitaxy: InAs QD's form on GaAs(001),[4] GaAs(113)*A* and *B*,[5,6] and GaAs(114)*A* and *B*,[6] whereas InAs grows in the layer-by-layer growth mode with the introduction of dislocations on GaAs(110),[7] GaAs(111)*A*,[8] and GaAs($\overline{111}$)*B*.[9] The differences in growth mode have not been explained yet. Presumably, the structure of the substrate surface influences the growth kinetics, producing specific QD sizes and size distributions.[5,10] Furthermore, the substrate orientation may induce certain bonding facets on the QD's and therefore determine their shape.[11–16] It is therefore interesting to compare the formation and development of InAs QD's on substrates of different orientation.

It has been reported already that InAs QD's on GaAs(001) exhibit two mirror-symmetry planes as on the bulk-truncated (001) substrate. From reflection high-energy electron diffraction (RHEED) observations a (136) orientation of the facets was proposed earlier.[11] Later and presumably more correctly, four (137) bounding facets were derived from scanning tunneling microscopy (STM).[13] These facets, which frame nearly the whole QD, grow with equal rates because of the same reconstruction and elastic energy density. On high-index substrates the symmetry is lower and, e.g., GaAs{113} surfaces exhibit only one symmetry plane normal to the surface. Therefore, only two planes are expected with equivalent indices and growth rates. As two planes alone cannot confine a 3D island, other surfaces with different growth rates are likely to develop. Thus, preferential migration of In atoms among the different bounding facets from the slower to the faster growing facets, so-called intersurface diffusion, should be taken into account.

In this contribution we report on the influence of substrate reconstruction and orientation on the shape, size, and size distribution of InAs QD's grown on GaAs(113)*A* (Refs. 17–19) and GaAs($\overline{113}$)*B* (Refs. 20 and 21) substrates. Generally, one defines the *A* and *B* faces as follows: A surface in the vicinity of (111)*A* is an *A* face, and a surface in the vicinity of ($\overline{111}$)*B* is a *B* face. Although we have already reported on the atomically resolved shape of these QD's,[14,15] we find it important to compare the growth on the two substrates in greater detail and to illuminate the role of the wetting layer. First, we show that the atomic arrangement is not the same on the bare GaAs{113} surfaces and on the subsequently grown InAs wetting layers. We conclude that this obviously induces a different morphological response to the misfit strain and results in different sizes and size distributions of the QD's. Second, we demonstrate from atomically resolved STM images that, although the bounding facets appearing on the main part of the QD's are identical, the overall shape of the QD's is largely different on both substrates.

In Sec. II we will give some experimental details. In Sec. III we will combine results and discussion for the bare substrate surface, the wetting layer, the coherent islands, called QD's, the larger islands, some of them being presumably incoherent, and their growth kinetics. We also will summarize the results for the atomically resolved shape of the majority, presumably coherent QD's. The conclusion will follow in Sec. IV.

II. EXPERIMENT

The experiments were carried out in a multichamber ultrahigh-vacuum system that was equipped with a molecular-beam epitaxy (MBE) and an STM chamber (Park Scientific Instruments, VP2) as described in detail elsewhere.[22] The GaAs(113)*A*- and GaAs($\bar{1}\bar{1}3$)*B*-oriented substrates with a typical size of 5×10 mm^2 were cut from a GaAs(113) wafer (*n* type, Si doped, carrier concentration $1.4–4.8\times10^{18}$ cm^{-3}, Wafer Technology) and prepared in the same way. The samples were cleaned by several ion bombardment and annealing cycles. Thereafter GaAs buffer layers about 50 nm thick were deposited using MBE at a sample temperature of 530–570 °C. The temperature was measured by a pyrometer that was calibrated against the GaAs(001) $c(4\times4)$ to (2×4) transition at 465 ± 10 °C. The samples were then cooled down to 450 ± 10 °C and InAs was deposited at a growth rate of about 0.05–0.07 Å /s and an As_2/In ratio of 40–50 at an As_2 pressure of 7×10^{-7} mbar. The deposition of 2.5 ± 0.3 ML ($ML_{113}=1.82$ Å ; the index 113 indicates the monolayer perpendicular to {113}) of InAs onto GaAs(113)*A* and of 1.7 ± 0.3 ML onto GaAs($\bar{1}\bar{1}3$)*B* led to the appearance of sharp spots in the RHEED pattern (with the electron beam along $[33\bar{2}]$), indicating the onset of 3D SK growth. Immediately after the transition to the SK growth, the samples were transferred to the STM chamber within 60 s without breaking the vacuum. STM images were acquired from the uncapped QD's at room temperature in constant-current mode.

III. RESULTS AND DISCUSSION

A. Bare GaAs(113)*A* and GaAs($\bar{1}\bar{1}3$)*B* surfaces and InAs wetting layers

At 450 °C — the growth temperature of the InAs QD's — the bare GaAs(113)*A* surface exhibits the (8×1) reconstruction [it is called "8×1" with respect to the face-centered (113) unit cell].[17–19] It was confirmed by RHEED patterns during preparation, afterwards at room temperature, and also through subsequent STM experiments at room temperature. Zigzag chains of As dimers extending along $[\bar{3}\bar{3}2]$ are characteristic elements of this reconstruction as depicted schematically in Fig. 1(a). The GaAs(113)A(8×1) reconstruction[17–19] comprises three atomic layers with an overall corrugation of 3.4 Å and exhibits the largest unit cell among the known GaAs reconstructions: 32.0 Å in the $[\bar{1}10]$ direction and 13.3 Å in the $[\bar{3}\bar{3}2]$ direction. The zigzag chains in the top and middle layers are phase shifted by a quarter of the unit cell in $[\bar{3}\bar{3}2]$ direction. Note that a surface, formed by continuously stacking zigzag chains from middle to top to next top and so on, results in a (3 7 15) surface.[23] Between the middle zigzag chains in the (8×1) unit cell there is a trench containing As and Ga dangling bonds from the third layer. The bulk-truncated (113) surface exhibits $(\bar{1}10)$ as symmetry plane, but the (8×1) reconstruction suspends this symmetry. A small-area STM image of GaAs(113)*A* is presented in Fig. 1(b). We succeeded in atomically resolving the As dimers in the zigzag chains. The overall corrugation measured from STM images is 3.0 ± 0.4 Å and the length of unit cell vectors is 32.5 ± 0.5 Å and 13.0 ± 0.5 Å , which nicely confirms the model for the (8×1) reconstruction.

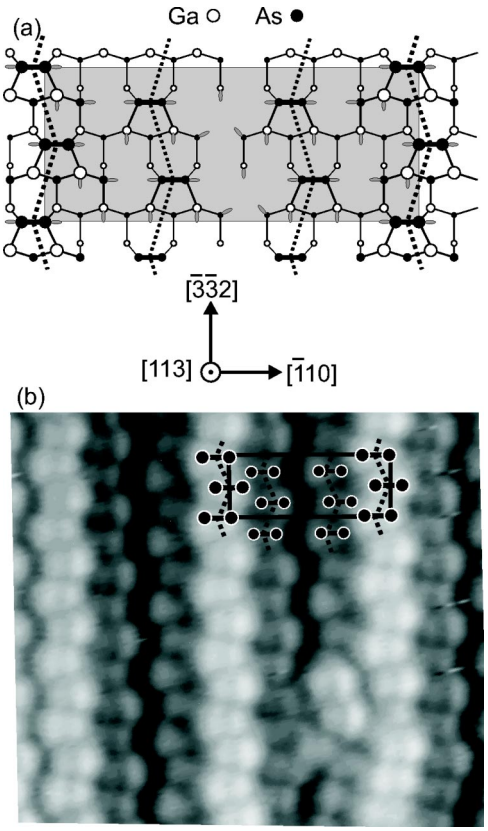

FIG. 1. (a) Top view of the structural model for GaAs(113) $A(8\times1)$. Atoms in the second and third layers are depicted with smaller circles. The As atoms in dimers are connected with black bars. The zigzag chains of As dimers are depicted with dotted lines. (b) Atomically resolved STM image of GaAs(113)$A(8\times1)$: the size of the image is (90×80) Å^2, sample bias voltage $U=-2.5$ V, sample current $I=0.24$ nA. In the overlay As dimers are depicted with black circles and connected by dotted lines in accord with the structural model.

Several authors have reported on an unusual undulating morphology on GaAs(113)*A*, both for surfaces prepared by MBE and by metal-organic vapor phase epitaxy.[24–26] In Ref. 24 it has been shown that GaAs(3 7 15)*A* and GaAs(2 5 11) *A* surfaces appear as side facets of arrowhead like pits, surrounded by the (8×1) reconstruction. This was not reproduced in the present study. (The difference may be due to the buffer layer which was about 200 nm in the former studies compared to 50 nm in the present work.) Under the preparation conditions in this study the surface consists of fairly small (8×1) terraces with many islands up to 12 Å in height and up to 180×600 Å^2 in lateral dimensions, which are seen in Fig. 2(a) as large hills elongated in the $[\bar{3}\bar{3}2]$ direction. (The stripes along $[\bar{3}\bar{3}2]$ are due to the As-dimer zigzag chains.) The density of the hills is $(3.7\pm1.5)\times10^{10}$ cm^{-2}, which is of the same order of magnitude as

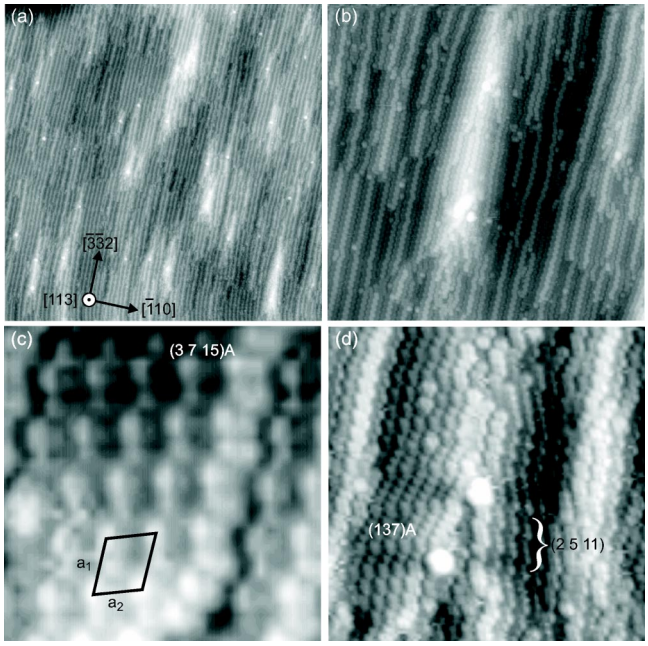

FIG. 2. (a) Overview STM image of GaAs(113)*A*(8 × 1): (2620 × 2620) Å^2, $U=-2.5$ V, $I=0.16$ nA. (b) High-resolution STM image of GaAs(113)*A*(1 × 1) with a 3D GaAs island: (685 × 685) Å^2, $U=-2.5$ V, $I=0.16$ nA. (c) High-resolution STM image of the GaAs(3 7 15)*A*(1 × 1) facet on the GaAs islands: (74 × 74) Å^2, $U=-2.5$ V, $I=0.16$ nA. (d) High-resolution STM image of the spike of a GaAs island on GaAs(113)*A*(8 × 1): (230 × 230) Å^2, $U=-2.7$ V, $I=0.2$ nA.

the density of subsequently grown InAs QD's. Thus, these GaAs islands may act as nucleation centers for the InAs QD's: For the first few layers of InAs overgrowing the GaAs island, strain relaxation on top of the island is more efficient than in a homogeneous InAs layer. This effect is similar to the mechanism responsible for strain-induced vertical stacking of InAs QD's on GaAs(001),[27] where the lattice of the embedding material is expanded around the buried dot i.e., the local lattice constant is nearer to that of the growing InAs, and therefore the QD's in the next layer of the stack prefer to form at these areas of expanded substrate lattice.

A magnified STM image of a typical GaAs island is shown in Fig. 2(b). On both sides of the island, {3 7 15}*A* facets develop along [$\bar{3}\bar{3}2$] by stacking of (8 × 1) As-dimer zigzag chains. A high-resolution STM image of one of the facets is shown in Fig. 2(c). The facet is inclined to the (113)*A* substrate by 9 ± 3° and exhibits the unit cell vectors $a_1=13.2\pm0.3$ Å and $a_2=11.0\pm0.5$ Å . [The geometrical values for the GaAs(3 7 15)(1 × 1) reconstruction projected onto the (113) plane are 9.7°, 13.3 Å , and 10.5 Å , respectively.] The size of each facet is up to 100 unit cells. As the islands have a triangular shape, facets other than (3 7 15) should develop as bounding facets. The {137}*A* (Ref. 13) and {2 5 11}*A* (Refs. 23,24 and 28) surfaces, whose intersection lines with the (113)*A* surface are tilted against [$\bar{3}\bar{3}2$] by 16.8° and 5.7°, fulfill this requirement and were actually found in this region, as shown in Fig. 2(d). However, no long-range-ordered areas of these surfaces were observed.

The appearance of high-index GaAs{3 7 15}*A*, {137}*A*, and {2 5 11}*A* surfaces on GaAs(113)*A* cannot be explained by the surface free energy, because under As-rich conditions the respective values of 55 meV/Å^2 (Ref. 28), 56 meV/Å^2 (Ref. 29), and 53 meV/Å^2 (Ref. 28) are greater than the value of 47 meV/Å^2 which was calculated for the GaAs(113)*A*(8 × 1) reconstruction.[18] Probably, the shape of the GaAs islands is influenced by growth kinetics, which was found to be very anisotropic on {113} surfaces.[17,19]

The (113)*A* surface becomes more corrugated and even disordered when depositing InAs. The large-area STM image of the InAs wetting layer on GaAs($\bar{1}\bar{1}3$)*A* in Fig. 3(a) reveals that the 3D hills elongated along [$\bar{3}\bar{3}2$] still remain, with a slightly decreased density $< 10^{10}$ cm^{-2}, and the height and lateral dimensions are less well defined. An atomically resolved STM image in Fig. 3(b), acquired from the wetting layer between the large hills, shows the disappearance of any flat region on the surface. Poorly ordered, small arrowhead like hills develop instead of the original (8 × 1) reconstruction. The 3D hills are pointing along [$\bar{3}\bar{3}2$] with walls built up from a mixture of {3 7 15}*A*, {2 5 11}*A*, and {137}*A* surfaces. [In Fig. 3(c) a (137)*A* facet is shown.] A similar behavior of the wetting layer was observed by depositing $In_{0.5}Ga_{0.5}As$ onto GaAs(311)*A*.[30]

The strong undulation of the wetting layer is probably caused by a partial relaxation of the strain at the 3D hills so that a surface rich with hills may be favorable. Also, from the surface-energy point of view, covering the GaAs surface by InAs is favorable since the surface free energy of InAs(3 7 15)*A*, (2 5 11)*A*, and (137)*A* is 42, 41, and 44 meV/Å^2, respectively,[29] i.e., lower than for the respective GaAs surfaces. This difference in surface energy certainly favors, at least at the beginning, a 2D growth of the wetting layer and a smooth following of every substrate roughness. However, no long-range-ordered areas of these surfaces were observed after InAs deposition. Overall, the wetting layer exhibits a rather chaotic morphology.

Now we turn to the ($\bar{1}\bar{1}3$)*B* substrate which — during growth at high temperature — exhibits a well-ordered (8 × 1) reconstruction [as on the *A* side, 8 × 1 is taken with respect to the face-centered ($\bar{1}\bar{1}3$) unit cell] consisting of zigzag chains of Ga dimers in the top and middle layers,[13,21] obviously in an identical arrangement as the As dimers on the (113)*A* face for the As-rich (8 × 1) reconstruction. It can be recognized from Fig. 4 that the mesoscopic morphology of the GaAs($\bar{1}\bar{1}3$)*B*(8 × 1) surface differs strongly from that of the *A* face shown in Fig. 2; large terraces are observed and no tendency to form other high-index surfaces is recognized. This may be related to a presumably high energy of ($\bar{3}\,\bar{7}\,\bar{15}$)*B*,($\bar{2}\,\bar{5}\,\bar{11}$)*B*, and ($\bar{1}\bar{3}\bar{7}$)*B* surfaces which have not been observed up to now.

At 470–490 °C under As_2 flux, the GaAs($\bar{1}\bar{1}3$)*B* surface undergoes a transition to a less-ordered (2 × 1)+(1 × 1) structure by incorporating As atoms and rearranging Ga dimers, thus filling up the trenches. This mixed (2 × 1) +(1 × 1) structure consists of locally ordered As adatoms and dimers on the bulk-truncated ($\bar{1}\bar{1}3$)*B* surface.[21] Thus, at

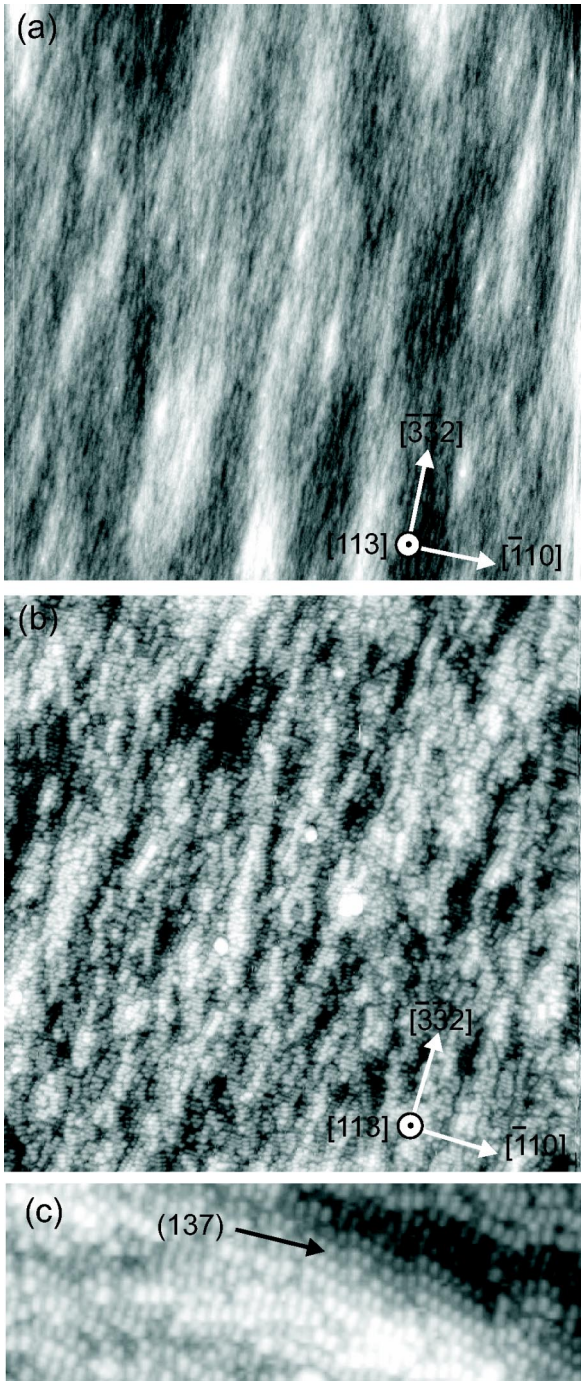

FIG. 3. STM images of the InAs wetting layer on GaAs(113)*A*. The thickness of deposited InAs is 1.85 ML. (a) (4000 × 4000) Å^2, $U=-3.0$ V, $I=0.5$ nA; (b) (1000 × 1000) Å^2, $U=-3.0$ V, $I=0.2$ nA; (c) turned by 90° with respect to (a) and (b) (480 × 165) Å^2, $U=-3.0$ V, $I=0.2$ nA.

450 °C — the growth temperature of the InAs QD's — the surface reconstruction is not the same as on the GaAs(113)*A* substrate. Furthermore, with the transition to the As-rich phase, the GaAs($\overline{1\,1\,3}$)*B* surface does not change its morphology.[21]

STM images of the InAs wetting layer (see one example in Fig. 5) exhibit terraces up to 1000 Å wide, separated by

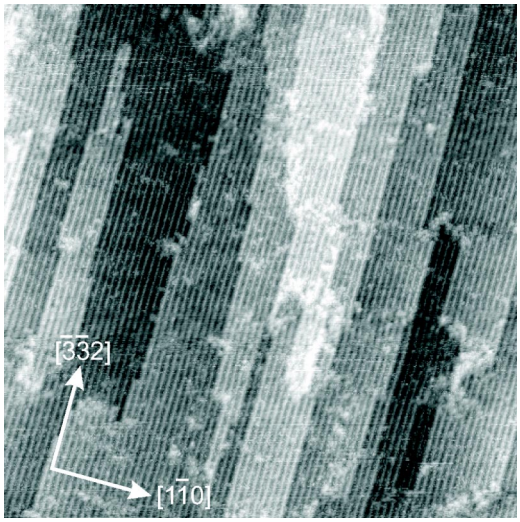

FIG. 4. Overview STM image of GaAs($\overline{1\,1\,3}$)*B*(8 × 1): (2500 × 2500) Å^2, $U=-2.8$ V, $I=0.15$ nA. The surface was prepared — following buffer layer growth — by keeping the sample at the growth temperature of 530°C for 15 min and the As_2 Knudsen cell shut off, i.e., under less As-rich conditions. From Ref. 21.

mostly monatomic steps; i.e., the ($\overline{1\,1\,3}$)*B* substrate remains very flat before the growth of InAs QD's starts. Moreover, near to the SK transition, as is the case in Fig. 5, the morphology is very similar to that on (001) (Ref. 31): small (S) and large (L) 2D monatomic islands and small 3D clusters (C) up to 4 ML in height (potential precursors for the InAs QD's) are seen in the STM image. One may suppose that the very large similarity and the rather flat wetting layer may be mirrored in the similarly favorable optical properties found for InAs QD's grown on both the GaAs(001) (Ref. 32) and the GaAs($\overline{1\,1\,3}$)*B* (Ref. 33) substrate.

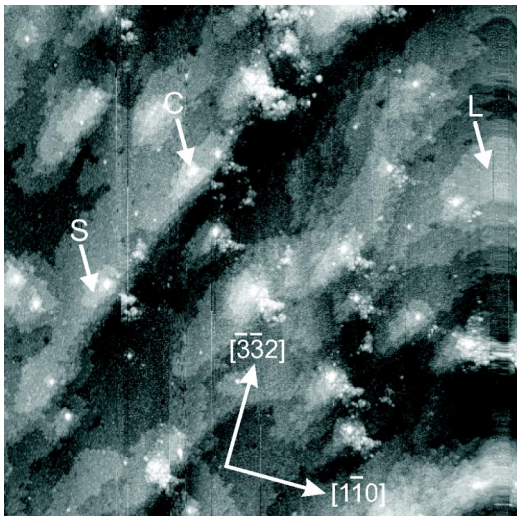

FIG. 5. Overview STM image of the InAs wetting layer on GaAs($\overline{1\,1\,3}$)*B*(8 × 1) just before the SK transition: (4000 × 4000) Å^2, $U=-2.55$ V, $I=0.1$ nA. The thickness of deposited InAs is 1.35 ML.

B. Kinetic interrelation between the shape of individual QD's and the statistical properties of QD ensembles

The development in time of a QD ensemble consists of two periods, which may, for different QD's of the ensemble, also overlap: a nucleation period and a growth period, in which the QD's acquire their final size. In the following, we will attempt to show that the relative duration of both periods is crucial for the properties of the resulting QD's. Growth proceeds by adding layers of material to the side facets of the QD's. The duration of the growth period is determined by the magnitude of diffusive flow of material from the wetting layer to the QD's, but more importantly by the speed of 2D growth of the fastest-growing facet of the QD. Due to the latter effect, the shape of the individual QD's in an ensemble and the statistical properties of the ensemble, in particular the sharpness of the QD size distribution, are interrelated.

We will first discuss the QD shape: Due to the different 2D growth speed of different QD facets, a characteristic growth shape of the QD's evolves. For an object of convex geometry, such as a QD, fast 2D growth of a facet leads to elongation of the QD in the direction of this facet, and finally the facets will disappear from the QD. The remaining facets grow more slowly, and thus the overall growth rate of the QD will become smaller and smaller, until growth stops when all available InAs has been consumed. The relative growth speed of facets can be estimated from growth experiments on patterned substrates.[34–38] However, one should keep in mind that certain facets, on the patterned substrate or on the quantum dot or on both, may grow in step-flow mode, with the edge between two facets acting as a continuous source of steps. In this case, the detailed atomic structure of the edge and its reactive properties may be crucial for deciding the relative growth speed of the two adjacent facets.

Next we will discuss the size of the QD's: While earlier calculations for InAs QD on GaAs(001) have shown that there is no energetic reason for a specific island size to be reached[39] (an island may grow indefinitely by decreasing its average energy per atom), several reasons lead to a slowing down of the growth and, finally, to a rather well-defined island size. First, there is only a finite amount of InAs available, in which a given number of nuclei must share. This leads to a well-defined value for the average island size.[40,41] Second, large QD's tend to grow more slowly, and therefore the QD's in an ensemble tend to end up at similar sizes. There is a number of effects contributing to this rather general trend: As pointed out in the paragraph above, on larger islands, only the more slowly growing facets remain. Moreover, if the growth of a facet does not proceed in step-flow mode, a 2D nucleus must be formed on the facet each time a new layer is added. It has been argued that the activation energy for forming such a nucleus increases with the size of the facet.[42] Consequently, facet growth stops once the QD has reached a certain size. Furthermore, it has been shown, at least in a special case, that the strain field induced in the substrate around a QD hinders diffusive material flow towards the dot.[43] Since the strain field of a QD is inhomogeneous, with the highest strain values at the footing of the QD, in the center of the edge between QD and substrate (see Ref. 42), large QD's are affected more strongly by the detrimental effect of strain on surface diffusion. All these effects together give rise to a quite well-defined size of the QD's, at which their growth stops or at least becomes very slow.

Under these premises, the size distribution in an ensemble of QD's is determined by the relative duration of the nucleation period and growth period. The time scale for the nucleation period is set by the amount of supersaturation supplied by the flux of In atoms and by their diffusivity on the surface. Furthermore, in the case of heterogeneous nucleation, the number and availability of special nucleation sites will affect the duration of the nucleation period. The duration of the growth period depends mainly on the speed at which the growing QD's can incorporate the material, i.e., on the growth speed of the fastest-growing facet. If 3D growth of the QD's is rather fast, but nucleation proceeds over a longer period, the ensemble will — at each moment — consist of QD's at different stages of their growth. We call this nucleation limitation. On the other hand, if nucleation is limited to a rather narrow time interval compared to the time scale of QD growth, the final size of an individual QD will be almost independent of the moment of its nucleation, and the QD ensemble will exhibit a narrow size distribution, for the reasons discussed above. We call this growth limitation. In the following, we will compare the experimental findings for QD's grown on the GaAs(113)*A* and $(\overline{113})B$ substrate with the above considerations in mind.

C. Comparison of the QD ensembles GaAs(113)*A* and GaAs $(\overline{113})B$

Different atomic structures of the bare GaAs(113)*A* and GaAs surfaces and the respective InAs wetting layers let us suppose that somewhat different QD's may develop on these two surfaces. Indeed, some well-defined differences were observed experimentally. Figure 6 shows two STM images for InAs QD's grown on GaAs(113)*A* and GaAs$(\overline{113})B$ in a 3D plot. More detailed views from on top are given in Fig. 7. From Figs. 6 and 7 one recognizes that on (113)*A* three different structures can be observed: small hills or embryo dots, a larger number of QD's of intermediate size, and several larger islands. Both the QD's and the larger dots are extended along $[33\overline{2}]$. An embryo dot is marked by an arrow in Fig. 6(a) and also depicted below in Fig. 9(a). The embryo dot is terminated by {2 5 11}*A* surfaces which are inclined to the substrate by only 10.0°.

So on the GaAs(113)*A* substrate it seems that dots in different growth states are observed. Such a situation is expected for nucleation limitation, i.e., if nucleation takes place over a period typical for QD growth. We have already speculated that the QD's may grow on top of the hills in the rough substrate layer. As these hills have random sizes and different built-in strains, the critical InAs thickness will be exceeded locally at different moments during the InAs deposition. This means that events of nucleating QD's will take place over a rather long time interval.

The behavior on $(\overline{113})B$ is remarkably different. The wetting layer is much more smooth and the ensemble of dots much more uniform. Besides the normal QD's, only a small

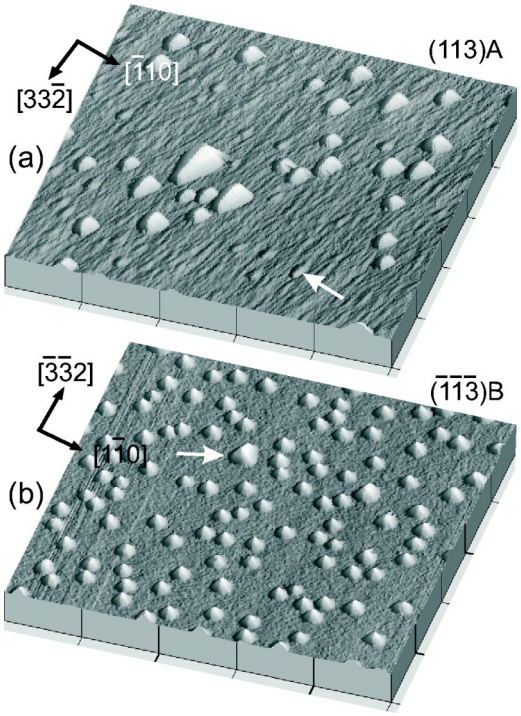

FIG. 6. 3D overview STM images of the InAs QD's grown on the (a) GaAs(113)*A* and (b) GaAs($\overline{113}$)*B* surfaces. The images were acquired and presented in 3D form with the same parameters: The size is (5000 × 5000) Å^2, $U=-3$ V, $I=0.1$ nA. The growth temperature was 450 °C and the nominal InAs thickness was 2.5 ML_{113} on the *A* and 1.4 ML_{113} on the *B* face. A nucleus on the (113)*A* surface and a large dot are marked by arrows.

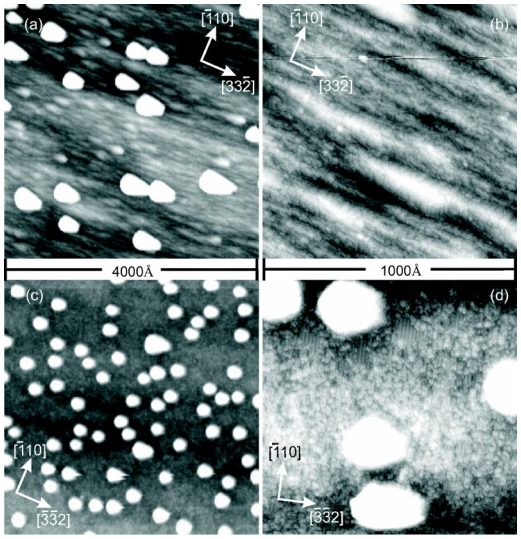

FIG. 7. (a) Top-view STM images of InAs QD's on GaAs(113)*A*. (b) Dot embryos and wetting layer for InAs QD's on GaAs(113)*A*. (c) Top-view STM images of InAs QD's on GaAs($\overline{113}$)*B*. (d) Wetting layer for InAs QD's on GaAs($\overline{113}$)*B*. $U=-3$ V, $I=0.1$ nA.

number of elongated dots is observed. One of them is marked by an arrow in Fig. 6(b). Remarkable is also the different structure in the wetting layer as already discussed above. So for ($\overline{113}$)*B* we conclude that we are in a growth regime different from the (113)*A* surface: The nucleation period is short compared to the growth period, and the finally observed QD ensemble does not preserve any memory of nucleation. No small dots or embryos can be observed under these conditions, as can be clearly seen in Figs. 7 (c) and 7(d). These observations provide clear evidence for the above-mentioned growth limitation.

The critical thickness — as established with RHEED — at which the 3D QD's are formed is 2.5 ± 0.3 ML_{113} for the *A* face and 1.7 ± 0.3 ML_{113} for the *B* face. The delay in the SK transition on the *A* face can be explained by the partial relaxation of InAs at the 3D small and large hills observed already on the wetting layer, because in the 3D structures InAs can better relax than in the 2D film. A similar delay of QD formation was found for $In_{0.5}Ga_{0.5}As$ grown by the MBE for GaAs(311)*A* compared to GaAs(100) under otherwise identical preparation conditions.[30]

The different size distributions of the QD's are apparent: While there are many small as well as large dots on the *A* face, those on the *B* face are very uniform. The measured size distributions are shown in Fig. 8. On the (113)*A* surface, the measured diameters at the base along [$\overline{332}$] are distributed between 30 and 60 nm with the peak of 35% at 40 nm and between 20 and 40 nm with the peak of 45% at 30 nm on the ($\overline{113}$)*B* surface. The 3 × 10^{10} cm^{-2} in number density on GaAs($\overline{113}$)*B* is higher than the 9.5 × 10^9 cm^{-2} on GaAs(113)*A*. Before we compare the QD formation on the *A* and *B* faces in further detail, we briefly recall the atomically resolved shape of the individual QD's as determined by *in situ* STM images of unburied dots.[14,15]

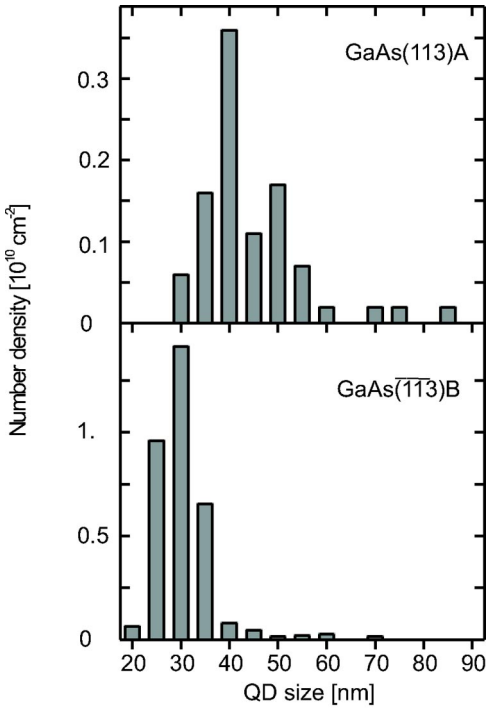

FIG. 8. Size distribution for QD's grown on GaAs(113)*A* and ($\overline{113}$)*B* substrates at 450 °. The full width at the base along [$\overline{332}$] was taken.

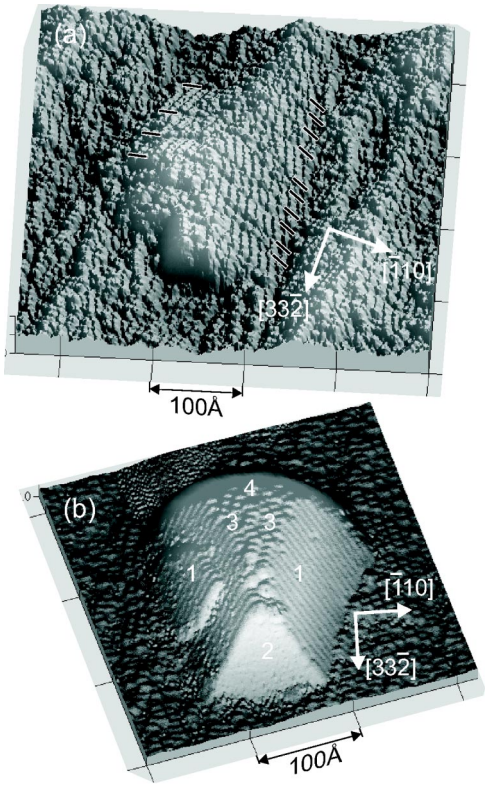

FIG. 9. (a) 3D STM image of a QD nucleus grown on GaAs(113)*A*: (440 × 440) Å^2, $U=-3.0$ V, $I=0.1$ nA. The stripes of {2 5 11}A facets are indicated by the bars at the nucleus foot. (b) 3D STM image of an InAs QD of an intermediate shape: (320 × 320) Å^2, $U=-3.0$ V, $I=0.32$ nA.

D. Atomically resolved shape of InAs QD's on GaAs(113)*A*

It is fascinating how perfectly crystalline islands form on the disordered wetting layer on the GaAs(113)*A* surface shown in Fig. 3(b). Figure 9(a) exhibits an atomically resolved embryo dot which will be discussed below. Figure 9(b) presents a 3D STM image of an typical InAs QD with a height of 45 Å .[15] It adopts an intermediate shape between the embryo in Fig. 9(a) and the elongated island in the final growth state (see Fig. 12 below). The exact azimuthal directions on the substrate were determined from the atomically resolved wetting layer as well as from wafer-manufacturer data. The QD exhibits mirror symmetry with respect to the $(\bar{1}10)$ plane perpendicular to the (113)*A* substrate plane along $[33\bar{2}]$. The island comprises two symmetrical facets 1, a frontal facet 2, two small facets 3 on the summit, and a rounded region 4.

The facets 1, shown in Fig. 10(a) on an enlarged scale, are identified to be {110} planes from following STM measurements: The facets are inclined to the (113)*A* substrate by 29° ± 4° and exhibit unit-cell vectors of $u_1=3.8\pm0.2$ Å and $u_2=5.5\pm0.2$ Å . [The geometrical values for the InAs(GaAs){110} surface projected onto (113) are 31.5°, $u_1=3.9(3.6)$ Å , and $u_2=5.8$ (5.4) Å , respectively.] On the left facet 1 in Fig. 9(b) [on the (101) surface] a 2D embryo, 1 ML high, can be seen that occupies the lower middle part of the facet. In the theory outlined in Refs. 39 and 42, it has been assumed that nucleation occurs at the bottom edge, which is at first glance in agreement with our observation. However, these calculations had shown that nucleation at the lower facet edge, in particular in the middle of this edge, would be associated with high strain energy i.e., the InAs material must be strongly compressed before incorporation into the QD crystal. Therefore the authors of Refs. 39 and 42 assumed that the 2D embryo grows out of one of the lower corners of the facet. Our observation shows that this assumption is not generally valid, thus casting some doubt on the details of the growth model considered in Refs. 39 and 42. The observation of such an island further indicates that the (110) facets grow rather slowly; otherwise, a full facet layer would have been developed during shutting off the Knudsen cells.

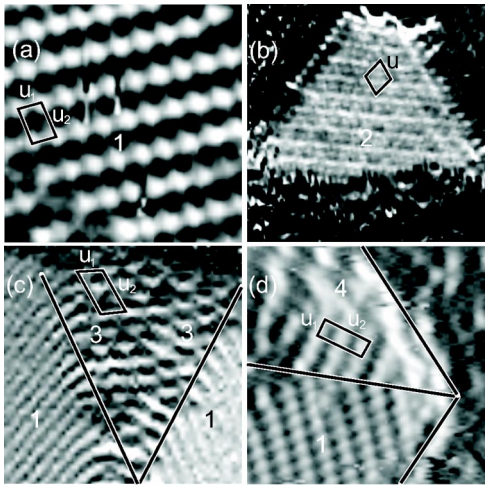

FIG. 10. Atomically resolved STM images (error signal = constant-height mode) of corresponding facets on the QD, numbered in Fig. 9(b): (a) the (011) or (101) facet: (37 × 37) Å^2, $U=-3.1$ V, $I=0.135$ nA; (b) the (111)$A(2\times2)$ reconstructed facet: (98 × 98) Å^2, $U=-3$ V, $I=0.32$ nA; (c) (2 5 11)$A(1\times1)$ reconstructed facets on the summit of the island: (110 × 110) Å^2, $U=-2.5$ V, $I=0.33$ nA; and (d) the border between the (011) and the $(\bar{1}\bar{1}3)B(1\times1)$ facet: (63 × 63) Å^2, $U=-3.1$ V, $I=0.135$ nA.

The triangular facet 2 [Fig. 10(b)] is a (111)$A(2\times2)$-reconstructed surface as derived from following measurements: It is inclined to (113)*A* by 26° ± 4° and exhibits a rhombic unit cell with the vector $u=8.0\pm0.4$ Å . [Geometrical values for the In(Ga) vacancy buckling model of the (111)$A(2\times2)$ reconstruction[44,45] are 29.5° and $u=7.8$ (7.2) Å .] The filled-state STM image in Fig. 10(b) is also very similar to that acquired from the planar GaAs(111)$A(2\times2)$ surface.[46]

The facets 3 on the summit of the island [Fig. 10(c)] are {2 5 11}*A*-reconstructed surfaces as extracted from the following measurements: The angle to the substrate and the lengths of the unit-cell vectors are 7 ± 3°, $u_1=11.5\pm0.5$ Å , and $u_2=21.7\pm1.0$ Å , respectively. [The geometrical values for the InAs(GaAs) {2 5 11}$A(1\times1)$ reconstruction[23,28] are 10.0°, $u_1=11.3$ (10.5) Å , and $u_2=20.2$ (18.8) Å .] The small {2 5 11}*A* facets are characteristic of an intermediate stage during QD growth and disap-

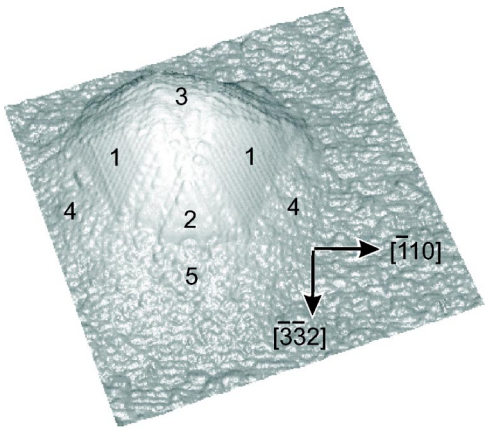

FIG. 11. 3D STM image of an InAs QD grown on GaAs($\overline{113}$)*B* with five characteristic regions: (420 × 420) Å^2, $U=-3$ V, $I=0.1$ nA. From Ref. 14.

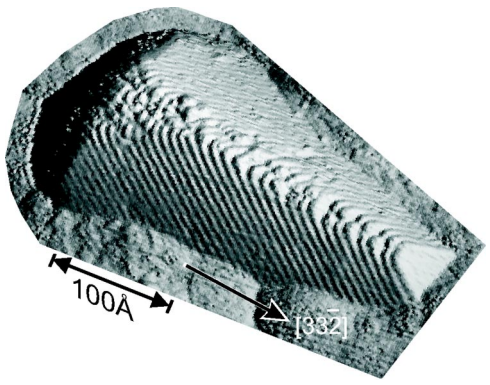

FIG. 12. 3D STM image of an elongated InAs QD grown on GaAs(113)*A*: $U=-2.5$ V, $I=0.33$ nA. From Ref. 15.

pear when the QD achieves the final elongated shape (see below). We note that very large (2 5 11)A facets were observed on top of the InAs QD's on GaAs(113)*A* by Wang *et al.*[16] We believe that the difference with our results is in the different As_2 pressure which was larger by an order of magnitude in Ref. 16. The surface free energy of the (110) cleavage plane (52 meV/Å^2) is independent of the chemical potential of As_2,[53] whereas the surface energy of the GaAs(2 5 11)*A*(1 × 1) reconstruction increases towards Ga-rich conditions. This means that — similar to the GaAs surfaces — the difference between energies of both surfaces was larger in the present study and therefore the InAs(2 5 11) facets vanished from the QD's leaving behind the InAs{110} facets.

Region 4 in Fig. 9(b) exhibits a complex structure, which appears to be rounded on the intermediate islands. In the simplest case, the (001) surface, inclined to (113)*A* by 25°, could develop in this area. The rounded shape must be attributed to a sequence of crystal planes vicinal to (001) or, equivalently, to a (001) surface with many irregular atomic steps that cannot be atomically resolved in STM. The high step density is indicative of a high growth speed in this region.

E. Atomically resolved shape of InAs QD's grown on GaAs ($\overline{113}$)*B*

Only two types of islands are observed on GaAs($\overline{113}$)*B*: many relatively small QD's of remarkably uniform size and some large islands with very broad size distribution.[14,47] A typical InAs QD is depicted in Fig. 11. Similar to the (113)*A* case the QD is mirror symmetric with respect to the ($\bar{1}$10) plane normal to the substrate. The QD comprises a steep main part terminating by regions 1, 2, and 3 and a flat base consisting of facets 4 and 5. The flat base, which was not observed on the QD's on GaAs(113)*A*, is an intrinsic part of the InAs QD's on GaAs($\overline{113}$)*B*, which appears not only during growth, but still exists after annealing treatment of the samples.[47]

As described in Ref. 14, two symmetrical facets 1 and the triangular facet 2 from the main part were identified to be {110} and ($\overline{111}$)*B*($\sqrt{19}$ × $\sqrt{19}$) surfaces, respectively. Similar to the QD's on GaAs(113)*A* a rounded structure develops also on the backside 3 of the island on GaAs($\overline{113}$)*B*, which was considered to be composed of a stacking of vicinal (00 $\bar{1}$) surfaces. The flat base consists of facets 4 and 5, inclined to ($\overline{113}$)*B* by 14.5° and 10.0°, which were determined to be of {$\overline{135}$}*B* and {$\overline{112}$}*B* orientation, respectively.

The existence of the flat base is in agreement with the idea, proposed in Ref. 15, that the growth rate is lower on those facets where the As-As bond of As_2 has to be broken before incorporation. We will come back to this point below. The {$\overline{112}$}*B* and {$\overline{135}$}*B* facets connect the {110} and ($\overline{111}$)*B*($\sqrt{19}$ × $\sqrt{19}$) facets with the GaAs($\overline{113}$)*B* substrate. The latter three faces actually do not exhibit As dimers at the reconstructed surface. Also, the edges between them and ($\overline{113}$)*B* substrate do not supply sites, where As_2 molecules an be incorporated without dissociation. We speculate that this could delay the incorporation of In atoms from the wetting layer onto {110} and ($\overline{111}$)*B* facets, while In presumably reacts with As adatoms and forms low-energy ($\overline{112}$)*B* and {$\overline{135}$}*B* surfaces at the island foot. In contrast, the rounded region of vicinal (00$\bar{1}$) surfaces can grow with As_2. Therefore, no connecting facet develops between this region and the GaAs($\overline{113}$)*B* substrate. More generally, difficulties with the incorporation of As_2 molecules may also be responsible for the above-discussed growth limitation on the GaAs ($\overline{113}$)*B* substrate.

F. Large InAs islands grown on GaAs(113)*A*

About 60% of all measured InAs QD's grown on GaAs(113)*A* adopt a final shape elongated along [33$\bar{2}$] that is shown in Fig. 12. The elongation, observed also by several other groups,[5,48] gives rise to a spatial anisotropy of the luminescence light, which can be applied in polarization-sensitive devices.[49] In comparison to the QD in Fig. 9(b), there is a drastic reduction in size of the (111)*A* facet: The length of the edge between (111)*A* and (113)*A* decreases from (116 ± 30) Å for the intermediate QD to (60 ± 20) Å

for the elongated QD's. This infers that (111)*A* is a fast-growing facet where In and As are incorporated relatively easily. As a consequence, new (111)*A* layers are added quickly, causing this facet to vanish and leaving behind increasing {110} facets on both sides of the island. An analysis of the shape of several large islands with different sizes clearly shows that the larger islands have grown almost exclusively in the $[33\bar{2}]$ direction, while the opposite rounded side of the islands grows only little. Instead, there is a further faceting of the rounded (001) region with appearance of $(\bar{1}\bar{1}3)B$ facets.

Why is an elongation scenario realized instead of proportional growth of the rather round, intermediate shape shown in Fig. 9(b)? We believe that there is a connection between retarded growth of the rounded side and the appearance of the $(\bar{1}\bar{1}3)B$ facets on it. Generally, the (001) facet grows with the largest rate as reported in experiments of simultaneous growth of low-index surfaces on patterned GaAs substrates,[34–38] whereas other facets on the QD's on GaAs(113)*A* grow rather slowly. We would expect the growth rate of the rounded region to be increased further by the high step density on the vicinal (001) surface. When the islands adopt the final shape, elongated along $[33\bar{2}]$ (see below), the vicinal (001) region partially transforms into two flat surfaces, which were identified to be $(\bar{1}13)B$ and $(1\bar{1}3)B$ facets. They form well-ordered edges with the {110} facets as shown in Fig. 10(d). The $(\bar{1}13)B$ or $(1\bar{1}3)B$ surface is inclined to (113)*A* by $40° \pm 5°$ and exhibits the unit-cell vectors $u_1 = 4.1 \pm 0.2$ Å and $u_2 = 13.0 \pm 0.3$ Å . [The geometrical values are 35.1°, $u_1 = 3.9$ (3.6) Å , and $u_2 = 13.7$ (12.8) Å (Ref. 50)].

In contrast to the epitaxy on GaAs(001), where the As_2 molecules can be incorporated as As dimers,[51] for the growth of GaAs$(\bar{1}\bar{1}3)B$, the As_2 molecules must always be dissociated.[52] Very likely, the occurrence of $(\bar{1}\bar{1}3)B$ facets decreases the growth rate at the rounded region strongly since breaking the As-As bonds of the incoming As_2 molecules requires some additional energy. Owing to the — with respect to $[\bar{1}10]$ — larger diffusion length in the $[33\bar{2}]$ direction,[35] the In atoms are then incorporated mainly at the (111)*A* facet. We note here that the edge of the (111)*A* facet with the (113)*A* substrate allows for incorporation of As_2 molecules without dissociation. This is indicated schematically in Fig. 13: In our model two In atoms are adsorbed at the edge whereby a bond of an As surface dimer is broken. These two In atoms together with two In atoms from the (111)*A* facet can bond an As_2 molecule without dissociation as a new dimer. This dimer may be broken up by further In atoms and a new layer on the (111)*A* facet starts to grow. As a result of the fast growth of the (111)*A* facet the QD adopts the elongated shape.

G. Large InAs islands grown on GaAs$(\bar{1}\bar{1}3)B$

Only 4% of all islands on GaAs$(\bar{1}\bar{1}3)B$ adopt a somewhat elongated shape shown in Fig. 14. Contrary to the elongated QD's on GaAs(113)*A* there is no reduction of the GaAs facet size. The length of the edge between the $(\bar{1}\bar{1}1)B$ and $(\bar{1}\bar{1}2)B$ facets even increases from 105 ± 15 Å for the QD's to 120 ± 15 Å for the elongated islands. This behavior indicates that the growth of the elongated shape, if it occurs, proceeds mainly by the growth of the $(00\bar{1})$ rounded region

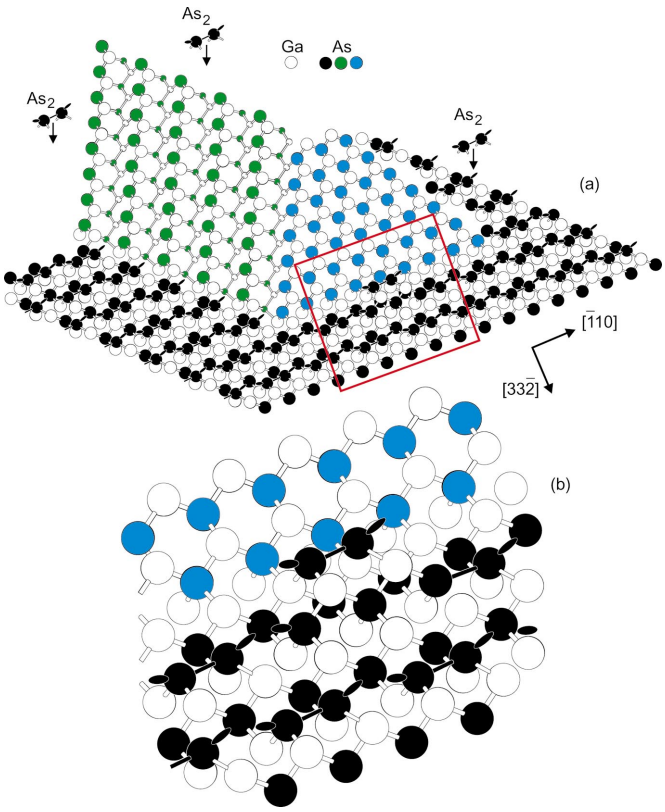

FIG. 13. (Color) (a) Ball-and-stick model of one corner of the InAs QD grown on GaAs(113)*A*. The As atoms are marked in different colors: black for the (113)*A* substrate, blue for the (111)*A* facet of the QD, and green for the (101) facet of the QD. Also a first growth nucleus at the edge between the (113)*A* substrate and (111)*A* facet is depicted. (b) Enlarged part at the edge between the (111)*A* facet and the substrate derived from (a).

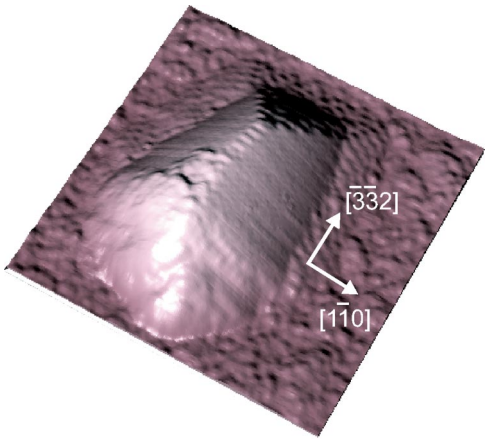

FIG. 14. 3D STM image of an elongated InAs QD grown on GaAs$(\bar{1}\bar{1}3)B$: (420 × 420) Å^2, $U = -3$ V, $I = 0.1$ nA.

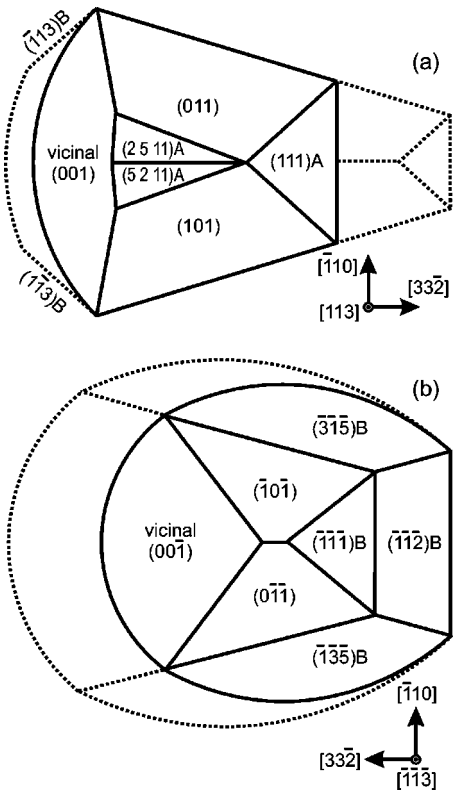

FIG. 15. Shape of InAs QD's derived from STM measurements: (a) a QD on GaAs(113)*A*. The solid line represents the intermediate QD shape, and the dotted line shows final elongated QD's after further growth. (b) A QD on GaAs($\overline{113}$)*B*. The solid line indicates the shape of the QD and the dotted line the incoherent island elongated along [33$\overline{2}$].

in the [33$\overline{2}$] direction. However, similar to the QD's on the *A* face, the {113}*A* facets should develop on the (00$\overline{1}$) vicinal region. In fact, a strong decrease of the growth rate at the rounded region and a flattening of the rounded region by the formation of {113}*A* facets is not observed in the STM images of the elongated islands. This may be due to a difference in growth rate between the (113)*A* and ($\overline{113}$)*B* facets.

The size distribution of the elongated islands[47] is very broad with the lengths along [33$\overline{2}$] from 450 up to 850 Å. There is also no report about a polarization anisotropy from elongated QD's on GaAs($\overline{113}$)*B*. These facts suggest that these islands are incoherent, i.e., have one or several dislocations incorporated at the interface to the substrate which relieve the strain. Incorporating the dislocation requires to surmount an energetic barrier, and this is achieved only in a few cases (experimentally, 4% of all islands are found to be elongated). After the dislocation has been formed, the (00$\overline{1}$) region can grow with the largest rate without limitation caused by elastic strain present in the QD's, as reported for simultaneously growing low-index surfaces on patterned GaAs substrate.[36,37] The islands become elongated along [33$\overline{2}$]. In Fig. 15 the models for the intermediate and the elongated QD on (113)*A* and ($\overline{113}$)*B* are sketched.

H. Discussion of growth kinetics

Because of its highly disordered, undulating morphology, the (113)*A* surface very likely exhibits an inhomogeneous strain distribution just before the SK transition. The small and large hills, protruding from the wetting layer, observed in Fig. 3(a), can be considered as places where the strain is better relieved and may serve as nucleation sites. Since the height and lateral dimensions of the hills are not equal, the QD growth processes after the SK transition may proceed not simultaneously on the whole surface. Evidence for this may be found in the embryo aside from the mature QD's as can be seen in Fig. 6(a). These effects are responsible for the observed broad size distribution on the (113)*A* substrate typical for nucleation limitation. Such a behavior has not been reported yet for the InAs/GaAs heteroepitaxy on other substrate orientations.

Besides the QD's and the presumably incoherent islands we also observe growth embryos on the (113)*A* surface. Figure 9(a) shows an STM image of a typical embryo. We have positioned this image very early in this presentation in order to facilitate the comparison with the mature QD in Fig. 9(b). The embryos have a triangular shape elongated towards [$\overline{33}$2] with the height up to 13 Å . The bounding facets are inclined to the substrate by $8° \pm 4°$ and exhibit the stripe like structure with the width of three As dimers, which is characteristic for the {2 5 11}*A* surfaces[23,28] [the geometric angle between {2 5 11} and (113) planes is 10.0°]. However, the {2 5 11}*A* facets are fairly disordered; also narrower and wider stripes [marked in Fig. 9(a)] are seen on the nucleus. Interestingly, the QD's start to grow with very flat, stable low-energy surfaces, e.g., {2 5 11}*A* in the present case; i.e., the misfit strain drives the system not immediately into a more steeper shape.

The islands on the (113)*A* surface are terminated by {2 5 11}*A* surfaces when they start growing from the wetting layer. Since {2 5 11} is terminated by As dimers, it may grow fast following the argument given above. Similarly to the fast growing (111)*A* facet later in the growth process, the {2 5 11} *A* facets disappear from the QD's, whereas the slower growing {110} facets remain and increase in size. As {110} facets are energetically more favorable, a shape nearer to equilibrium is reached later in the growth process.

For the ($\overline{113}$)*B* surface we suggest another growth scenario: Since the wetting layer on the ($\overline{113}$)*B* substrate is rather flat, the strain is distributed homogeneously on the whole surface. Therefore, the probability of the QD formation is equal everywhere so that a simultaneous SK transition takes place. After the SK transition the QD's starts to grow almost simultaneously with a similar growth rate. This is one prerequisite for obtaining the narrow size distribution that is observed on GaAs($\overline{113}$)*B*. Nucleation can only occur initially in a time interval short compared to the typical growth time of a dot. This has been noted above as growth limitation.

It is obvious from Fig. 6 that the shape of the QD's grown on GaAs(113)*A* and GaAs($\overline{113}$)*B* is quite different: A larger number of islands on the (113)*A* substrate are elongated to-

wards $[33\bar{2}]$, whereas the islands on the *B* face are mostly rather round. According to our interpretation outlined above this results from the distinctive differences in nucleation and growth which very likely are induced by the differences in the respective wetting layers. The InAs/GaAs system waits for a theoretical simulation which would deliver the hierarchy of atomistic processes and the rate determining steps. Our study on the (113)*A* surface is especially interesting for this purpose since it exhibits many different growth states: embryos, intermediate (coherent) QD's and large (presumably coherent as well as incoherent) islands. Interestingly on both substrates, the area from which the material is collected seems not to play a role in determining the size of the QD's: There are areas free of QD's whereas in other areas QD's are rather near to each other as can be seen from Figs. 6(b) and 7(c).

IV. CONCLUSION

We have compared the growth of InAs QD's on GaAs(113)*A* and GaAs$(\bar{1}\bar{1}3)B$ substrates. The symmetry of the QD's and orientation of the main bounding facets are found to be equal on both GaAs(113)*A* and GaAs$(\bar{1}\bar{1}3)B$ substrates. The QD's on GaAs(113)*A* exhibit $(\bar{1}10)$ as symmetry plane, {110} and (111)*A* bounding facets, and a rounded region of the vicinal (001) surfaces. The latter region becomes more steep with the appearance of $(\bar{1}\bar{1}3)B$ surfaces in a later growth state, giving rise to a shape elongated along $[33\bar{2}]$. The QD's on GaAs$(\bar{1}\bar{1}3)B$ exhibit also the $(\bar{1}10)$ symmetry plane. $\{\bar{1}\bar{1}0\}$ and $(\bar{1}\bar{1}\bar{1})B$ and a rounded region of vicinal $\{001\}$ surfaces serve as bounding facets. Contrary to the QD's on GaAs(113)*A*, steeper $(\bar{1}\bar{1}3)$ *B* facets do not develop at the vicinal $\{00\bar{1}\}$ surfaces and a flat base of high-index $(\bar{1}\bar{1}2)B$ and $(\bar{1}35)B$ surfaces develops at the foot of the {110} and $(\bar{1}\bar{1}\bar{1})B$ bounding facets. So although the bounding facets appearing on the main part of the QD's are identical, the overall shape of the QD's is largely different on both substrates. The differences in shape are considered to be an effect of facet growth kinetics associated with As_2 molecule dissociation.

The morphology and atomic structure of the wetting layer also seem to have an important influence on QD formation. For the GaAs(113)*A* surface, the intrinsic undulation becomes much more pronounced with depositing InAs. The roughness of the wetting layer seems to hinder diffusion. The result is a very inhomogeneous strain distribution that may inhibit a SK transition simultaneous on the whole surface. It induces a broad size distribution of the InAs QD's. Furthermore, dot embryos are found, indicating rather late nucleation events. We observe here a clear case of nucleation limitation: Nucleation takes place at the same time scale as the growth itself.

The behavior on the GaAs$(\bar{1}\bar{1}3)B$ surface is quite different. The flatness of the GaAs$(\bar{1}\bar{1}3)B$ surface remains also after InAs deposition. Therefore, the QD growth starts simultaneously at the SK transition and the QD's grow with equal rates, resulting in a homogeneous size distribution.[47] Here we observe a case of growth limitation. Since the SK transition is rather short in time, we are unable to observe embryo dots.

Finally we like to underline that the GaAs(113)*A* substrate offers an unique opportunity to follow the kinetics of the QD growth, from the nuclei to the mature elongated islands. This system is very appropriate for future growth simulations.

ACKNOWLEDGMENTS

We thank G. Ertl for support and P. Geng for technical assistance. T.S. thanks the Alexander von Humboldt Foundation for a support. The work was supported by the Deutsche Forschungsgemeinschaft (Grant No. SFB296, Project No. A2).

*Corresponding author. FAX:+49-30-8413-5106. Electronic address: jacobi@fhi-berlin.mpg.de

[1] Y. Masumoto and T. Takagahara, *Semiconductor Quantum Dots* (Springer, Berlin, 2002).

[2] D. Bimberg, M. Grundmann, and N. N. Ledentsov, *Quantum Dot Heterostructures* (Wiley, Chichester, NY, 1999).

[3] I. N. Stranski and L. Krastanow, Akad. Wiss. Wien, Math.-Naturwiss. Kl. Abt. 2A **146**, 797 (1937).

[4] D. Leonard, K. Pond, and P. M. Petroff, Phys. Rev. B **50**, 11 687 (1994).

[5] M. Henini, S. Sanguinetti, L. Brusaferri, E. Grilli, M. Guzzi, M. D. Upward, P. Moriarty, and P. H. Beton, Microelectron. J. **28**, 933 (1997).

[6] S. C. Fortina, S. Sanguinetti, E. Grilli, M. Guzzi, M. Henini, A. Polimeni, and L. Eaves, J. Cryst. Growth **187**, 126 (1998).

[7] J. G. Belk, J. L. Sudijono, X. M. Zhang, J. H. Neave, T. S. Jones, and B. A. Joyce, Phys. Rev. Lett. **78**, 475 (1997).

[8] H. Yamaguchi, M. R. Fahy, and B. A. Joyce, Appl. Phys. Lett. **69**, 776 (1996).

[9] S. E. Hooper, D. I. Westwood, D. A. Woolf, S. S. Heghoyan, and R. H. Williams, Semicond. Sci. Technol. **8**, 1069 (1993).

[10] S. Sanguinetti, G. Chiantoni, A. Miotto, E. Grilli, M. Guzzi, M. Henini, A. Polimeni, A. Patane, L. Eaves, and P C. Main, Micron. **31**, 309 (2000).

[11] H. Lee, R. Lowe-Webb, W. Yang, and P. C. Sercel, Appl. Phys. Lett. **72**, 812 (1998).

[12] Y. Hasegawa, H. Kiyama, Q. K. Xue, and T. Sakurai, Appl. Phys. Lett. **72**, 2265 (1998).

[13] J. Márquez, L. Geelhaar, and K. Jacobi, Appl. Phys. Lett. **78**, 2309 (2001).

[14] T. Suzuki, Y. Temko, and K. Jacobi, Appl. Phys. Lett. **80**, 4744 (2002).

[15] Y. Temko, T. Suzuki, and K. Jacobi, Appl. Phys. Lett. **82**, 2142 (2003).

[16] M. Wang, H. Wen, V. R. Yazdanpanah, J. L. Shultz, and G. Salamo, Appl. Phys. Lett. **82**, 1688 (2003).

[17] M. Wassermeier, J. Sudijono, M. D. Johnson, K. T. Leung, B. G. Orr, L. Daweritz, and K. Ploog, Phys. Rev. B **51**, 14 721 (1995).

[18] J. Platen, A. Kley, C. Setzer, K. Jacobi, P. Ruggerone, and M. Scheffler, J. Appl. Phys. **85**, 3597 (1999).
[19] L. Geelhaar, J. Márquez, and K. Jacobi, Phys. Rev. B **60**, 15 890 (1999).
[20] J. Márquez, L. Geelhaar, and K. Jacobi, Phys. Rev. B **62**, 9969 (2000).
[21] J. Márquez, L. Geelhaar, and K. Jacobi, Phys. Rev. B **65**, 165320 (2002).
[22] P. Geng, J. Márquez, L. Geelhaar, J. Platen, C. Setzer, and K. Jacobi, Rev. Sci. Instrum. **71**, 504 (2000).
[23] L. Geelhaar, Y. Temko, J. Márquez, P. Kratzer, and K. Jacobi, Phys. Rev. B **65**, 155308 (2002).
[24] K. Jacobi, L. Geelhaar, and J. Márquez, Appl. Phys. A: Mater. Sci. Process. **75**, 113 (2002).
[25] M. Pristovsek, H. Menhal, T. Wehnert, J.-T. Zettler, T. Schmidtling, N. Esser, W. Richter, C. Setzer, J. Platen, and K. Jacobi, J. Cryst. Growth **195**, 1 (1998).
[26] R. Nötzel, J. Temmyo, and T. Tamamura, Appl. Phys. Lett. **64**, 3557 (1994).
[27] H. Eisele, O. Flebbe, T. Kalka, C. Preinesberger, F. Heinrichsdorff, A. Krost, D. Bimberg, and M. Dähne-Prietsch, Appl. Phys. Lett. **75**, 106 (1999).
[28] L. Geelhaar, J. Márquez, P. Kratzer, and K. Jacobi, Phys. Rev. Lett. **86**, 3815 (2001).
[29] P. Kratzer (unpublished).
[30] P. O. Vaccaro, M. Hirai, K. Fujita, and T. Watanabe, J. Phys. D **29**, 2221 (1996).
[31] R. Heitz, T. R. Ramachandran, A. Kalburge, Q. Xie, I. Mukhametzhanov, P. Chen, and A. Madhukar, Phys. Rev. Lett. **78**, 4071 (1997).
[32] K. Nishi, R. Mirin, D. Leonard, G. Medeiros-Ribeiro, P. M. Petroff, and A. C. Gossard, J. Appl. Phys. **80**, 3466 (1996).
[33] A. Polimeni, M. Henini, A. Patanè, L. Eaves, P. C. Main, and G. Hill, Appl. Phys. Lett. **73**, 1415 (1998).
[34] X. Q. Shen and T. Nishinaga, J. Cryst. Growth **146**, 374 (1995).
[35] R. Nötzel, J. Menniger, M. Ramsteiner, A. Trampert, H.-P. Schönherr, L. Däweritz, and K. H. Ploog, J. Cryst. Growth **175/176**, 1114 (1997).
[36] A. Yamashiki and T. Nishinaga, J. Cryst. Growth **198/199**, 1125 (1999).
[37] S. Hirose, A. Yoshida, M. Yamaura, and H. Munekata, Appl. Phys. Lett. **74**, 964 (1999).
[38] D. Kishimoto, T. Nishinaga, S. Naritsuka, T. Noda, Y. Nakamura, and H. Sakaki, J. Cryst. Growth **212**, 373 (2000).
[39] N. Moll, M. Scheffler, and E. Pehlke, Phys. Rev. B **58**, 4566 (1998).
[40] L. G. Wang, P. Kratzer, M. Scheffler, and N. Moll, Phys. Rev. Lett. **82**, 4042 (1999).
[41] L. G. Wang, P. Kratzer, N. Moll, and M. Scheffler, Phys. Rev. B **62**, 1897 (2000).
[42] D. E. Jesson, G. Chen, K. M. Chen, and S. J. Pennycook, Phys. Rev. Lett. **80**, 5156 (1998).
[43] E. Penev, P. Kratzer, and M. Scheffler, Phys. Rev. B **64**, 085401 (2001).
[44] S. Y. Tong, G. Xu, and W. N. Mei, Phys. Rev. Lett. **52**, 1693 (1984).
[45] D. J. Chadi, Phys. Rev. Lett. **52**, 1911 (1984).
[46] Figure 1(b) in A. Ohtake, J. Nakamura, T. Komura, T. Hanada, T. Yao, H. Kuramochi, and M. Ozeki, Phys. Rev. B **64**, 045318 (2001).
[47] T. Suzuki, Y. Temko, and K. Jacobi, Phys. Rev. B **67**, 045315 (2003).
[48] H. Xu, Q. Gong, B. Xu, W. Jiang, J. Wang, W. Zhou, and Z. Wang, J. Cryst. Growth **200**, 70 (1999).
[49] M. Henini, S. Sanguinetti, S. C. Fortina, E. Grilli, M. Guzzi, G. Panzarini, L. C. Andreani, M. D. Upward, P. Moriarty, P. H. Beton, and L. Eaves, Phys. Rev. B **57**, R6815 (1998).
[50] Note that these values correspond to the bulk-truncated InAs-(GaAs)$(\overline{1}\overline{1}3)B(1 \times 1)$ surface (with respect to the face-centered rectangular unit cell). However, the (2×1) reconstruction with In dimers on the surface instead of the (1×1) reconstruction cannot be excluded, because the In dimers are invisible in filled-state STM images.
[51] P. Kratzer and M. Scheffler, Phys. Rev. Lett. **88**, 036102 (2002).
[52] T. Suzuki, Y. Temko, and K. Jacobi, Surf. Sci. **511**, 13 (2002).
[53] N. Moll, A. Kley, E. Pehlke, and M. Scheffler, Phys. Rev. B **54**, 8844 (1996).